J Therm Anal Calorim (2015) 122:47–53
DOI 10.1007/s10973-015-4722-x

Thermal properties and structure of zinc–manganese metaphosphate glasses

Jana Holubová[1] · Zdeněk Černošek[1] · Eva Černošková[2] · Ludvík Beneš[2]

Received: 9 January 2015 / Accepted: 19 April 2015 / Published online: 12 May 2015

Abstract The thermal properties and some physical characteristics of the metaphosphate glassy system xMnO–$(50-x)$ZnO–$50P_2O_5$ were studied. Homogeneous glasses were obtained in the whole concentration range between $Zn(PO_3)_2$ and $Mn(PO_3)_2$. The metaphosphate structure of the glasses was confirmed by Raman spectroscopy. The manganese was found to have a high-spin d^5-configuration in the glassy network, i.e., Mn(II), and the presence of a small amount of Mn(III) explained the purple color of the glasses, as confirmed by electron absorption spectroscopy. Thermoanalytical properties were studied by differential scanning calorimetry, thermomechanical analysis and differential thermal analysis. The phase diagram of the zinc–manganese metaphosphate system was proposed based on thermal analysis results and X-ray diffraction analysis of crystalline phases obtained after crystallization of undercooled melt. An eutectic composition was found close to 8 mol% MnO, while compositions with MnO content over 15 mol% form substitutional solid solutions. Some other properties as compositional dependence of glass transition temperature, thermal expansion coefficient and density were discussed on the basis of proposed phase diagram.

✉ Jana Holubová
jana.holubova@upce.cz

[1] Department of General and Inorganic Chemistry, Faculty of Chemical Technology, University of Pardubice, Studentská 573, 532 10 Pardubice, Czech Republic

[2] Joint Laboratory of Solid State Chemistry of Institute of Macromolecular Chemistry of Czech Academy of Sciences, v.v.i, University of Pardubice, Studentská 84, 532 10 Pardubice, Czech Republic

Keywords Zinc–manganese metaphosphate glasses · Thermal analysis · Phase diagram, Raman spectroscopy · XRD

Introduction

In the last few decades, phosphate glasses of various compositions have become much studied materials, in terms of both fundamental research and for their expected technological applications. Phosphate glasses offer an extremely wide range of possibilities for the tailoring of their physico-chemical properties for specific technological applications. These glasses have many desirable properties in comparison with silicate or borate glasses such as low melting temperature, high thermal expansion coefficient and transmission in an ultraviolet region [1–4]. As a result, phosphate glasses may find application in electronics and optics, in the hazardous waste immobilization and also have a number of biomedical applications [5–8].

Among the binary phosphate glasses, much attention has been paid to zinc phosphate glasses, mainly because of the unique structural role of ZnO, which can act as an intermediate oxide in the glass. As a glass former, it enters the network in the form of $[ZnO_4]$ structural units and can crosslink the phosphate chains by forming P–O–Zn bridges. As a glass modifier, Zn^{2+} ions occupy interstitial sites in the glass network [9–11]. Zinc metaphosphate glasses have attracted particular attention for their potential use in optical devices such as optical waveguides, glass–polymer composites and solid-state laser sources, and are often used as a seal between glassy and metallic parts [12, 13].

The introduction of transition metals such as manganese, molybdenum or tungsten, usually in multivalent states, into phosphate glasses induces structural changes and

causes interesting changes in their thermal, electrical, optical or magnetic properties [14–16].

Recently, glasses containing MnO have also been studied because manganese may be advantageously used as a paramagnetic probe to study the structure of phosphate glasses [17–19]. Manganese ions exist in different valence states in such glasses, namely as Mn^{2+} and Mn^{3+}, both with tetrahedral or with octahedral coordination in the glassy matrix. The study of zinc polyphosphate glasses doped with MnO by various methods has suggested that both Mn^{2+} and Mn^{3+} ions are present in these glasses and play a network modifier role [18, 19].

Great attention has been paid to mixed strontium–manganese metaphosphate glasses because of their photoluminescence properties, which make them promising materials for special optical applications. These glasses have been intensively studied by electron paramagnetic resonance, infrared and Raman spectroscopy techniques, and their optical, thermal and physical properties have been investigated in the light of the mixed alkali effect [20]. Study of the effect of manganese on the optical band gap of cadmium phosphate glasses has found that the optical band gap energy decreases with increasing manganese oxide content [21]. Lead niobium phosphate glasses containing small concentrations of manganese have also been studied, with the finding that the manganese ions existed mostly as Mn^{2+}, occupying network former positions in [MnO_4] structural units, and increased the rigidity of the glass network [22].

Phosphate glasses can be divided into several groups in terms of their P_2O_5 content and thus their content of basic phosphate structural units Q^0–Q^3 [3, 5]. Our attention was focused on the metaphosphate glasses with the PO_3^- basic structural unit, which were expected to have a wide glass-forming area owing to the known fact that metaphosphoric acid and its salts produce linear and cyclic polymer structures. The main objective of this work was to study the thermal properties of the metaphosphate glasses of xMnO–(50−x)ZnO–50P_2O_5 system with composition varying between both stoichiometric border compositions of zinc and manganese metaphosphate.

Experimental

Metaphosphate glasses of the ternary system ZnO–MnO–P_2O_5 having a gradual increase in MnO concentration were chosen for this study: xMnO–(50−x)ZnO–(50−x)P_2O_5, where $x = 0$, 2, 5, 7, 10, 20, 25, 40 and 50. Glasses were prepared by conventional melt-quenching method using ZnO and MnO (both 99.9 %; Sigma-Aldrich, Czech Republic), and H_3PO_4 (85 %, p.a.; Sigma-Aldrich). The appropriate amounts of the oxides and acid were mixed in platinum crucibles and heated slowly to 600 °C for approximately 2 h. The mixtures were then heated to 1100–1260 °C according to the manganese content and melted for 10 min at the final temperature in an electric furnace. The molten material was quenched at room temperature by pouring into a graphite mold, and the prepared glasses were slowly cooled to room temperature. Glass with $x = 50$ was also prepared with the addition of small amount of glucose as a reducing agent to maintain manganese in Mn(II) oxidation state.

Homogeneous glasses were prepared within the whole compositional range, and the amorphous nature of the samples was confirmed by X-ray diffraction (XRD). The chemical composition of the glasses was checked by X-ray fluorescence analysis (XRF; μ-XRF analyzer EAGLE II). The XRD measurements were performed on powdered samples using a D8 Advance diffractometer (Bruker) Cu K(α) radiation. The lattice parameters were calculated using EVA software, ver.19., Diffrac plus Basic Evaluating Package, Bruker AXS GmbH, Germany, 2013, and the error of monoclinic cell parameters a, b, c is ± 0,0004 Å, for cell angle β ± 0.005°.

The glass transition (T_g) of the samples was measured using a differential scanning calorimeter (DSC; Diamond, Perkin-Elmer) in the temperature region of 100–590 °C with heating rate of $q = 10$ °C min^{-1}. The softening temperature, T_d, and the thermal expansion coefficient of the samples were obtained by thermomechanical analysis using a TMA Q400 analyzer (TA Instruments). The measurements were made with a power of 0.050 N, and $q = 10$ °C min^{-1}. The thermal behavior of undercooled melts was studied by differential thermal analysis (DTA; SDT Q400; TA Instruments) within the temperature range 100–1100 °C and recorded at $q = 10$ °C min^{-1}. The coarsely crushed bulk samples were measured by both DTA/DSC techniques.

Raman spectra were recorded on bulk samples at room temperature using a LabRam HR Raman confocal microscope (Horiba Jobin–Yvon). The spectra were recorded in back-scattering geometry under excitation with a 532-nm Nd:YAG laser at a power of 5 mW.

Magnetic susceptibility measurements were made using a variable temperature Gouy balance system (Newport Instruments, UK).

The density of the glasses, ρ, was determined using the standard Archimedean method with toluene as the immersion liquid. The molar volume (V_m) of the samples was calculated according to the relation: $V_m = \bar{M}/\rho$, where $\bar{M}$ is the average molar weight of the glass.

Results and discussion

Basic characterization and oxidation states of manganese

The prepared basic glass 50ZnO–50P_2O_5 was colorless, and the color of the glasses changed from light purple to

very dark purple with increasing manganese content. This often observed purple color of phosphate, borophosphate or silicate glasses containing manganese is explained by the presence of Mn(III) in the glassy matrix [20, 22, 23]. Therefore, prior to further studies, it was necessary to confirm the oxidation state of the manganese in the glass samples.

Unambiguous determination of the oxidation state of manganese can be made using magnetic susceptibility measurements. The temperature-dependent magnetic susceptibility of selected glasses with different manganese concentrations was obtained, and the values of the effective magnetic moment, μ_{eff}, were calculated from the results. The obtained values were found to be independent of manganese concentration; the mean value was found to be $\mu_{eff} = 5.96\ \mu_B$. Based on the atomic magnetic moment values of free Mn^{2+} and Mn^{3+} ions (5.92 and 4.90 μ_B, respectively, [22]), it is possible to conclude that within the sensitivity of the method (±1 %), the manganese in the glasses has a high-spin d^5-configuration, i.e., Mn(II).

As known, Mn(II) has a d^5 electronic configuration, corresponding to a half-filled d shell, with the ground-level configuration $^6A_{1g}$. Because all excited states of Mn(II) are spin quartet states, all electronic transitions are parity and mainly spin forbidden according to the selection rules. Therefore, the intensity of the corresponding spectral bands is very low. However, the d^4 Mn(III) system has a ground level of ^5D, which splits into four states ($^5B_{1g}$, $^5A_{1g}$, $^5B_{2g}$ and ^5E_g) in octahedral crystal fields by Jahn–Teller distortion, leading to three spin-allowed electronic transitions. Figure 1 shows the ultraviolet–visible spectra of selected glasses. While the manganese-free glass showed no absorption in the visible range (curve 1), a broadband with a maximum at approximately 540 nm and a narrowband at 409 nm were observed in the spectra of glasses containing manganese (curve 2–4). The first absorption band results from the mixture of spin-forbidden electronic transitions of Mn^{2+} and the spin-allowed transitions of Mn^{3+} that are, however, much more intense. One of the latter ($^5B_{1g} \rightarrow {}^5B_{2g}$, ~530 nm) is responsible for the purple coloring of the glasses [20, 24]. Thus, it can be concluded that the coloration of the glasses was caused by the presence of Mn^{3+} in an amount below the sensitivity of magnetic susceptibility measurements. The band at 409 nm was attributed to the d–d transition of Mn(II) and is not significant to this discussion. The influence of Mn(III) on the color of the glasses was further confirmed after preparation of colorless glass with $x = 50$ in the presence of glucose as a reducing agent.

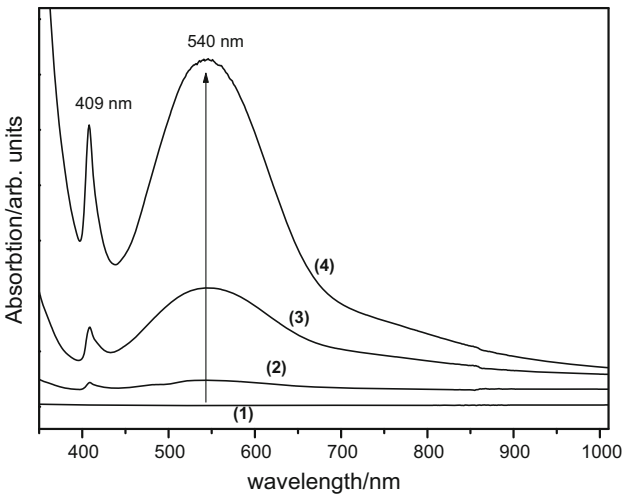

Fig. 1 Ultraviolet–visible spectra of xMnO–(50−x)ZnO–50P_2O_5 glasses of selected compositions $x = 0$ (1), $x = 2$ (2), $x = 20$ (3), $x = 50$ (4), for details see text

Raman spectra

The unchanged metaphosphate structure of the glasses across the whole compositional range was confirmed by Raman spectroscopy, as shown in Fig. 2. The spectrum of the MnO-free glass, 50ZnO–50P_2O_5, was dominated by two strong bands. The first was situated at 1207 cm^{-1} and can be assigned to the symmetric stretching vibration of terminal PO_2^- groups in Q^2 units. The second one at 703 cm^{-1} was caused by the symmetric stretching vibration of P–O–P bridges, the ν_s-POP mode, resulting in bending motion of the bridging oxygen [5]. The energies of these bands were slightly shifted toward lower wave numbers, to 1184 and 697 cm^{-1}, respectively, with increasing MnO content in the glass matrix. Besides the abovementioned bands, a weak feature observed at 1258 cm^{-1} was also slightly shifted to 1252 cm^{-1} with increasing Mn content. According to Ref. [9], this band arose from the coupling of stretching motions of terminal

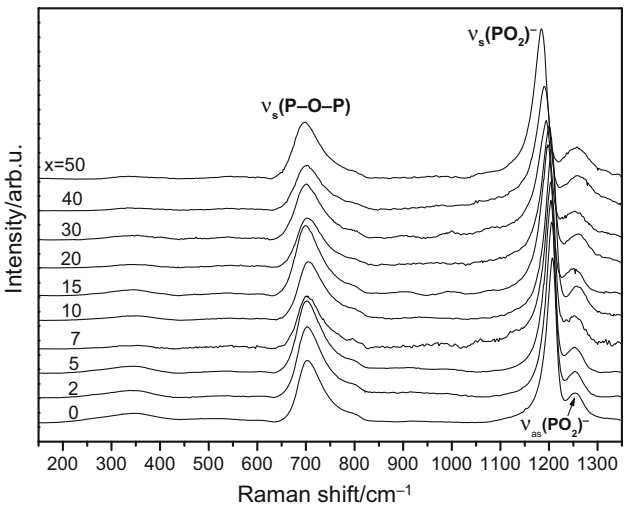

Fig. 2 Raman spectra of xMnO–(50−x)ZnO–50P_2O_5 glasses

(out-of-chain) and bridging (in-chain) oxygen atoms in metaphosphate units.

The above results unambiguously show that the glass structure was formed mainly by a metaphosphate network built up of Q^2 units in chain or ring arrangements.

Thermal analysis

Three thermoanalytical techniques were used to study the zinc–manganese metaphosphate glasses: (i) DTA of the glasses and their undercooled melts in the wide temperature range of interest, (ii) power-compensated differential scanning calorimetry (DSC) for precise measurement of the glass transition temperature, T_g, and (iii) thermomechanical analysis (TMA) to determine the softening temperature, T_d, and the thermal expansion coefficient, α, of the glasses. DTA curves of selected compositions are shown in Fig. 3, and the glass transition temperature region is magnified in inset.

Only one value of T_g was found for each glass changing between 410 and 470 °C, and thus, it can be concluded that the glasses were homogenous, see inset in Fig. 3. The compositional dependence of T_g is shown in Fig. 4 and can be divided into two regions. In the first, after an initial slight increase, T_g decreases with increasing concentration of MnO to its minimum at $x = 10$. In the second region (for $x > 10$), T_g increases practically linearly with MnO content. The compositional dependence of T_d showed a similar pattern.

Because the glass transition temperature reflects the rigidity of a glassy network, its increasing value with manganese concentration ($x > 10$) indicates an augmented cross-linking density and higher closeness of packing in the glassy network.

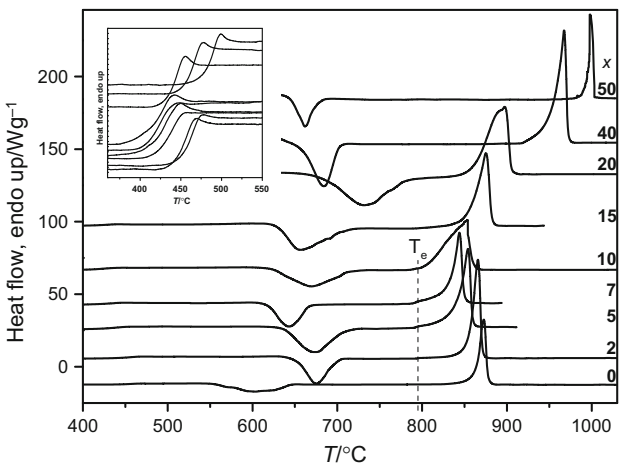

Fig. 3 DTA traces obtained for selected compositions; the magnified glass transition region is in the *inset*

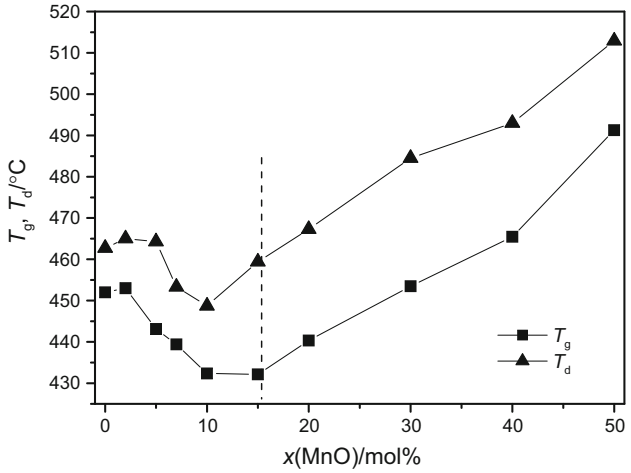

Fig. 4 Compositional dependence of the glass transition temperature, T_g, and softening temperature, T_d, of xMnO–(50−x)ZnO–50P_2O_5 glasses. *Error* in determination of both temperatures is lower than the point size

The behavior of undercooled melts was investigated by DTA owing to the need for measurements at temperatures above 600 °C, see Fig. 3. Only one crystallization peak was found on the DTA curves, in many cases nonsymmetric. The crystallization was followed by two endothermic effects. The first little intensive at 792 ± 4 °C was compositionally independent for composition up to $x \leq 15$, while at higher content of MnO its temperature gradually increased to the final temperature 997 °C. The temperature of the second peak gradually decreased to 792 °C for $x \leq 7$, and subsequently for samples with $10 \leq x \leq 50$, this temperature rose again to the final value 997 °C. It is, therefore, possible to conclude that the temperature 792 ± 4 °C is the eutectic temperature in the case of samples with $x \leq 15$.

The samples crystallized in the course of DTA measurement were studied by XRD, and obtained XRD pattern is shown in Fig. 5. XRD showed that only zinc metaphosphate (monoclinic, PDF No. 00-055-0130 [25]) crystallizes from undercooled melts up to 2 mol% of MnO and both zinc metaphosphate and manganese metaphosphate crystallize from melts with $2 < x \leq 15$. Above this MnO content, the crystalline phase with the structure derived from manganese metaphosphate structure was identified, and at the same time, the significant compositional change of unit cell parameters was observed, see the compositional dependence of cell parameters shown in Fig. 6. This indicates that in this compositional region, manganese progressively replaces zinc in any ratio forming thus substitutional solid solutions.

Based on both DTA and XRD results, the proposal of phase diagram of studied metaphosphate system was done, see Fig. 7. Proposed diagram is typical for binary system with partial solubility, and system under study can be

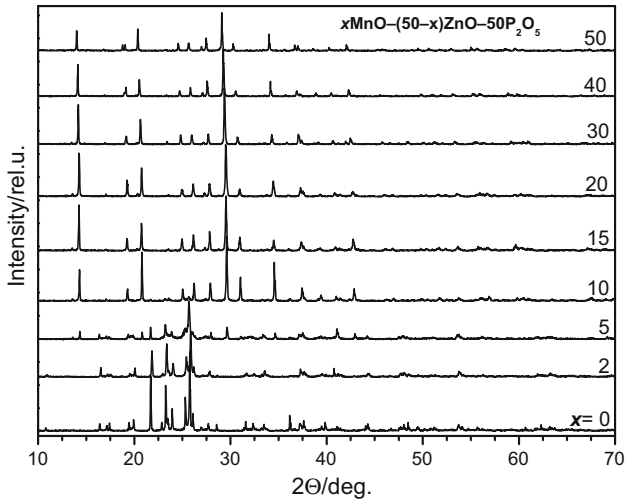

Fig. 5 XRD patterns of crystalline phases

characterized as a binary system $Zn(PO_3)_2$–$Mn(PO_3)_2$ with extremely narrow solid solution region on the $Zn(PO_3)_2$ side, see Fig. 7. The eutectic composition was estimated close to 8 mol% of MnO, and eutectic temperature is 792 °C. Above 15 mol% of MnO substitutional solid solutions are formed, wherein the zinc is progressively replaced by manganese in any ratio. It is possible to assume that from undercooled melts containing more than 15 mol% MnO, the compound, having a composition corresponding to the respective solid solution with the given ratio of manganese and zinc, crystallizes. This is consistent with the abovementioned compositional dependence of unit cell parameters of the obtained crystalline phases, Fig. 4. The final temperature 997 °C corresponds to the melting point of $Mn(PO_3)_2$. It should be noted that for the lowest concentration of MnO, the narrow region of solid solution exists (sketched by dashed line in Fig. 7), which could be responsible for nonmonotonic compositional dependencies of studied properties in this region, e.g., the glass transition or coefficient of thermal expansion. Determination of border of this region is below experimental resolution because preparation of the glasses with very low concentration of one of the components, MnO in our case, leads to the relatively great error of the glass composition.

The studied glasses can be divided into two groups according to the behavior of their undercooled melts, and this agrees well with compositional dependence of T_g, see Fig. 4. Glasses of the first group ($0 < x \leq 15$), which are characterized by a decrease of T_g, exhibited eutectic melting. Glasses of the second group ($x > 15$) with increasing T_g form solid solutions in which the zinc is replaced by manganese in any ratio.

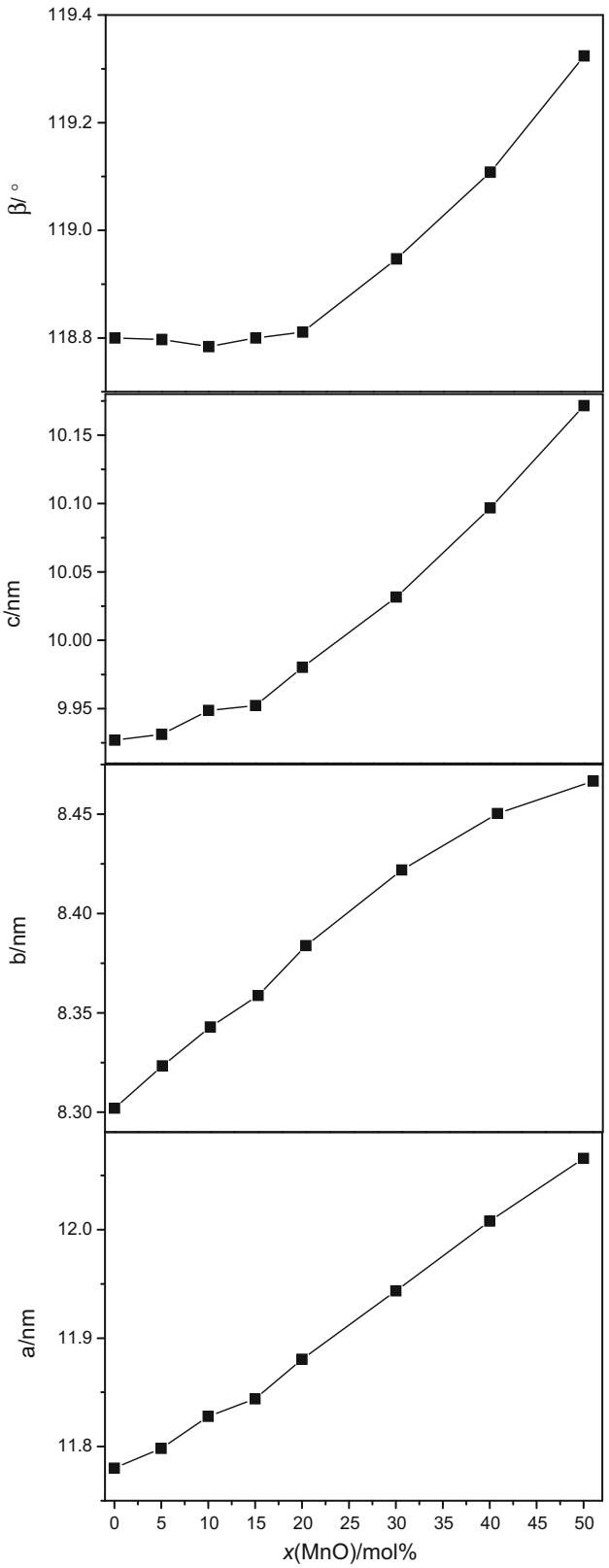

Fig. 6 Compositional dependence of the cell angle of the monoclinic crystalline phases

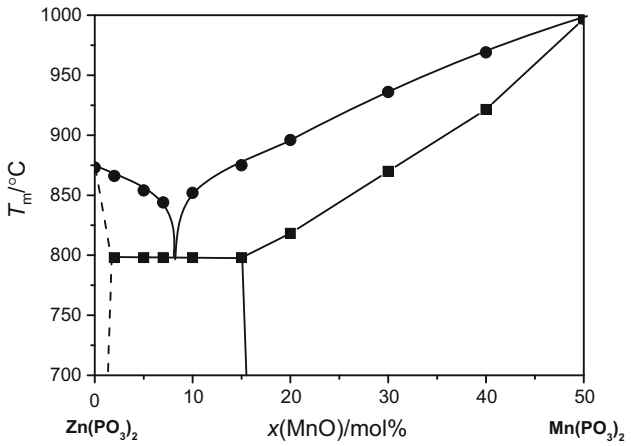

Fig. 7 Proposed phase diagram for the xMnO–(50−x)ZnO–50P_2O_5 glassy system

The thermal expansion coefficient, α, of glasses in the eutectic region did not exhibit monotonic concentration dependence, but increased almost linearly in the solid solution region (Fig. 8). This dependence corresponds well with the abovementioned phase diagram.

Density and molar volume

The density, ρ, of the studied glasses was measured by the common Archimedes method, and their molar volume, V_m, was calculated. Their compositional dependence is shown in Fig. 9. The density and molar volume varied nonlinearly with increasing manganese content, in agreement with the proposed phase diagram for this system. The breaks in the compositional dependencies are observed at compositions corresponding to the proposed eutectic point and the end of the eutectic region.

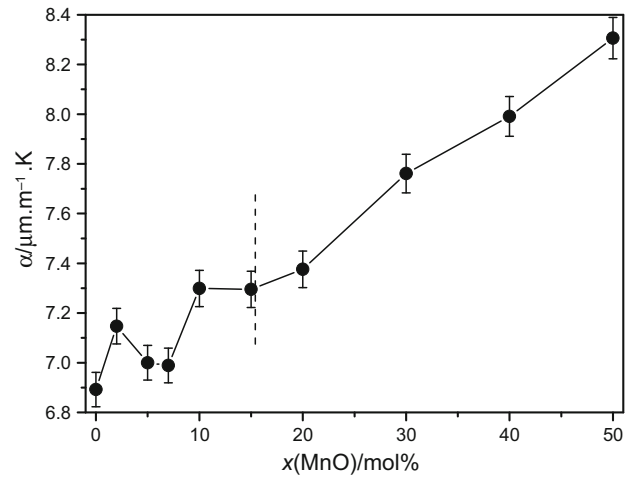

Fig. 8 Compositional dependence of the thermal expansion coefficient of the studied glasses; *curves* are only to guide the eye

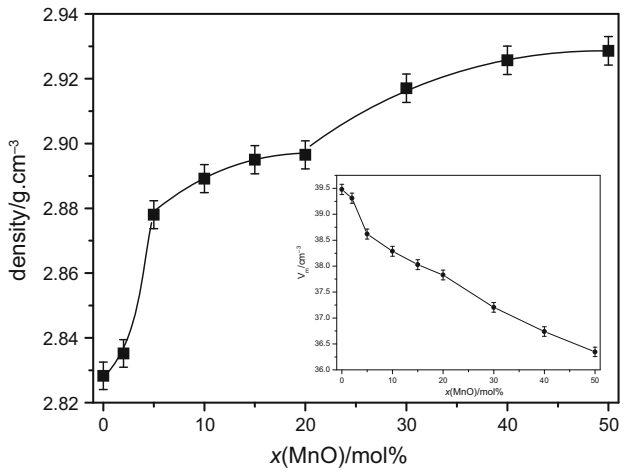

Fig. 9 Compositional dependence of the density and molar volume (*inset*) of xMnO–(50−x)ZnO–50P_2O_5 glass system; *curves* are only to guide the eye

Despite this nonlinear behavior, the density increased with Mn content, while V_m decreased (Fig. 9). The increase in density was surprising because the heavier zinc was replaced by the lighter and smaller manganese. This behavior can be explained by changes in the structure of the glassy network caused by substitution of four coordinated Zn with six coordinated Mn. This substitution led to an increase in the compactness of the structure that corresponded to the decrease in the calculated molar volume. These results are consistent with the conclusions drawn from the observed compositional dependence of T_g.

Conclusions

The thermal properties and some physical characteristics of the metaphosphate glassy system xMnO–(50−x)ZnO–50P_2O_5 were studied. Homogeneous glasses were obtained within the whole concentration range. Raman spectroscopy confirmed that the metaphosphate structure of the glassy network did not change as the content of MnO was increased. Magnetic susceptibility measurements showed that the manganese in the glassy network had a high-spin d^5-configuration, i.e., Mn(II), within the sensitivity of the method. The presence of a small amount of Mn(III) was confirmed by electron absorption spectroscopy and explained the purple color of the glasses.

Main attention was paid to the study of thermal properties of prepared glasses; obtained crystalline phases were also analyzed using XRD. On the basis of thermal analysis and XRD measurements, the zinc–manganese metaphosphate system was found to be typical pseudobinary system with partial solubility and the phase diagram of this system was proposed. The eutectic composition was found close to

8 mol% MnO with eutectic temperature 792 °C, while compositions with MnO content over 15 mol% form substitutional solid solutions. The compositional dependencies of the glass transition temperature, softening temperature, thermal expansion coefficient and density of glasses correlate well with this type of phase diagram.

References

1. van Wazer J. Phosphorous and its compounds, vol. 1 and 2. New York: Interscience; 1951.
2. Martin SW. Review of the structures of phosphate glasses. Eur J Solid State Inorg Chem. 1991;28:163.
3. Brow RK. Review: the structure of simple phosphate glasses. J Non-Cryst Solids. 2000;263&264:1–28.
4. Chromčíková M, Liška M, Macháček J, Šulcová J. Thermodynamic model and structure of $CaO–P_2O_5$ glasses. J Thermal Anal Calorim. 2013;114:785–9.
5. Brow RK, Alam MT, Tallant DR, Kirkpatrick J. Spectroscopic studies on the structure of phosphate sealing glasses. MRS Bulletin. 1998;23:63–67.
6. Ehrt D. Photoluminescence in the UV–VIS region of polyvalent ions in glasses. J Non-Cyst Solids. 2004;348:22.
7. Knowles JC. Phosphate based glasses for biomedical applications. J Mater Chem. 2003;13:2395–401.
8. Stoch P, Ciecinska M, Stoch A. Thermal properties of phosphate glasses for salt waste immobilization. J Therm Anal Calorim. 2014;117:197–204.
9. Tischendorf B, Utaigbe JU, Wiench JW, Pruski M, Sales BC. A study of short and intermediate order in zinc phosphate glasses. J Non-Cyst Solids. 2001;282:147–58.
10. Reddy MS, Krishna GM, Veeraiah N. Spectroscopic and magnetic studies of manganese ions in $ZnO–Sb_2O_3–B_2O_3$ glass system. J Phys Chem Solids. 2006;67:789–95.
11. Pascuta P, Borisi G, Jumate N, Vida-Semiti I, Vorel D, Culea E. The structural role of manganese ions in some zinc phosphate glasses and glass ceramics. J Alloys Compd. 2010;504:479–83.
12. Yang R, Liu H, Wang Y, Juany W, Hao X, Zhan J, Liu S. Structure and properties of ZnO-containing lithium–iron–phosphate glasses. J Alloys Compd. 2012;513:97–100.
13. Brow RK, Tallant DR. Structural design of sealing glasses. J Non Cryst Solids. 1997;222:396–406.
14. Mercier C, Palavit G, Montagne L, Follet-Houttemane C. A survey of transition-metal-containing phosphate glasses. C R Chem. 2002;5:693–703.
15. Chromčíková M, Liška M, Lissová M, Mošner P, Koudelka L. Structural relaxation of $PbO–WO_3–P_2O_5$ glasses. J Therm Anal Calorim. 2013;114:947–54.
16. Szumera M, Waclawska I. Thermal study of Mn-containing silicate–phosphate glasses. J Therm Anal Calorim. 2012;108:583–8.
17. Toloman D, Giurgiu LM, Ardelean I. EPR investigations of calcium phosphate glasses containing manganese ions. Phys B. 2009;404:4198–201.
18. Pascuta P, Bosca M, Borisi G, Cuela E. Thermal, structural and magnetic properties of some zinc phosphate glasses doped with manganese ions. J Alloys Compd. 2011;509:4314–9.
19. Kawamo M, Takebe H, Kuwabara M. Compositionals dependence of the luminescence properties of Mn^{2+}-doped metaphosphate glasses. Opt Mater. 2009;32:277.
20. Konidakis I, Varsamis C-PE, Kamitsos EI, Moencke D, Ehrt D. Structure and properties of mixed strontium–manganese metaphosphate glasses. J Phys Chem C. 2010;114:9125.
21. Altaj M, Chaudhry MA. Effect of MnO on the optical band gap in $Mno–CdO–P_2O_5$ glasses. J Korean Phys Soc. 2000;36:265–8.
22. Mohan NK, Reddy MR, Jayasankar CK, Veeraiah N. Spectroscopic and dielectric studies on MnO doped $PbO–Nb_2O_5–P_2O_5$ glass system. J Alloy Compd. 2008;458:66–76.
23. Moguš-Milankovic A, Pavic L, Srilatha K, Rao CS, Srikumar T, Sandhi Y, Veeraiah N. Electrical, dielectric and spectroscopic studies on MnO doped LiI-AgI–B_2O_3 glasses. J Appl Phys. 2012;111(1–11):013714.
24. Bartecki A, Burghess J, Kurza K. Colour of metal compounds. 2nd ed. The Netherlands: OPA (Overseas Publishers Association); 2000. p. 181.
25. Joint Committee on Powder Diffraction Standards, International Centre of Diffraction Data, Swarthmore, PA.